

This is the accepted manuscript made available via CHORUS. The article has been published as:

# Electrical transport properties of single-crystal $\text{CaB}_6$ , $\text{SrB}_6$ , and $\text{BaB}_6$

Jolanta Stankiewicz, Priscila F. S. Rosa, Pedro Schlottmann, and Zachary Fisk

Phys. Rev. B **94**, 125141 — Published 22 September 2016

DOI: [10.1103/PhysRevB.94.125141](https://doi.org/10.1103/PhysRevB.94.125141)

# Electrical transport properties of single crystals $\text{CaB}_6$ , $\text{SrB}_6$ and $\text{BaB}_6$

Jolanta Stankiewicz,<sup>1</sup> Priscila F. S. Rosa,<sup>2</sup> Pedro Schlottmann,<sup>3</sup> and Zachary Fisk<sup>4</sup>

<sup>1</sup>*Instituto de Ciencia de Materiales de Aragón and  
Departamento de Física de la Materia Condensada,  
CSIC–Universidad de Zaragoza, 50009-Zaragoza, Spain*

<sup>2</sup>*Department of Physics and Astronomy,  
University of California, Irvine, CA 92697,  
and Los Alamos National Laboratory,  
Los Alamos, New Mexico 87545, U.S.A.*

<sup>3</sup>*Department of Physics, Florida State University, Tallahassee, FL 32306, USA*

<sup>4</sup>*Department of Physics and Astronomy,  
University of California, Irvine, CA 92697, U.S.A.*

(Dated: September 2, 2016)

## Abstract

The electrical resistivity and Hall effect of alkaline-earth hexaboride single crystals are measured as a function of temperature, hydrostatic pressure and magnetic field. The transport properties vary weakly with the external parameters and are modeled in terms of intrinsic variable valence defects. These defects can stay either in (1) delocalized shallow levels or (2) localized levels resonant with the conduction band, which can be neutral or negatively charged. Satisfactory agreement is obtained for electronic transport properties in a broad temperature and pressure range, although fitting the magnetoresistance is less straightforward and a combination of various mechanisms is needed to explain the field and temperature dependence.

PACS numbers: 72.15.Qm, 75.20.Hr

## I. INTRODUCTION

Alkaline-earth hexaborides have attracted researchers' interest for over two decades. This has been triggered by the discovery of an unusual type of ferromagnetism in  $\text{CaB}_6$ <sup>1</sup> and  $\text{SrB}_6$ <sup>2</sup>. Neither the extensive theoretical and experimental work that followed on the electronic properties of  $\text{CaB}_6$ <sup>3</sup> nor more recent defect structure calculations<sup>4</sup>, experiments under pressure<sup>5-7</sup> and reports on structural and magnetic properties of nanocrystalline  $\text{CaB}_6$ <sup>8</sup> have led to a significantly deeper understanding of this intricate phenomena.

The continuing interest in hexaborides with cations of the alkaline-earth series ( $\text{AEB}_6$ ;  $\text{AE}=\text{Ca, Sr, Ba}$ ) stems also from the diverse behavior shown by this class of materials attributed to their native defects. The homogeneity range of the series is not easy to establish and most likely slight deviations from stoichiometry lead to some of the discrepancies encountered in many reports on the properties of  $\text{AEB}_6$ .

Divalent hexaborides have a simple cubic unit cell (a CsCl-type structure). Electronic structure calculations predict a sizable gap between the valence and the conduction band at the X-point in the Brillouin zone.<sup>9-11</sup> This has been corroborated by ARPES experiments on  $\text{CaB}_6$  and  $\text{SrB}_6$ .<sup>12,13</sup> In addition, a small electron-like spheroidal Fermi surface, centered at the X point, is seen in some of these studies.<sup>13</sup> Such observation is consistent with electrical transport properties which are usually found to be metallic, thus placing  $\text{AEB}_6$  at the boundary between semimetals and insulators. Experimental results show that the native defects are mainly donors, most likely brought about by cation vacancies or unintentional impurities.<sup>14-19</sup> In spite of many reports, a clear picture for electronic transport in alkaline-earth hexaborides is still lacking. Our aim is to establish a coherent pattern of electronic transport in these compounds.

The measured variation of the electrical resistivity and of the Hall effect with temperature, hydrostatic pressure, and magnetic field show the complexity of native donors in divalent hexaborides. Previously, we reported electrical resistivity and Hall effect behavior in  $\text{CaB}_6$  single crystals of different carrier concentrations. The temperature variation of these properties was accounted for by a model in which B-antisite defects (a Ca atom substituted by a B atom) were "amphoteric".<sup>20</sup> Here, we report results on an electronic transport study of  $\text{SrB}_6$  and  $\text{BaB}_6$ , in addition to  $\text{CaB}_6$ , single crystals. The electron concentration in these crystals spans three orders of magnitude, a much larger range than the one studied

before. This allows us to draw new conclusions about the nature of the native defects and their role in the transport properties of alkaline-earth hexaborides. In particular, we propose that these defects give rise to resonant levels within the conduction band. This idea was first introduced in solid state physics for metals,<sup>21</sup> but resonant levels occur in many semiconductors.<sup>22</sup> We have before suggested such an energy scheme for B-antisite defects in  $\text{CaB}_6$  but the explanation we now report differs from the previous one.

We hypothesize that each native donor gives rise to two types of electronic states: a delocalized shallow level and a more localized level, resonant with the conduction band, possibly emerging through lattice relaxation. In our relatively highly doped samples, a donor ion may also capture two electrons giving rise to negatively charged localized centers. The energy of the resonant levels is found to depend on electron concentration through mutual exchange and Coulomb interactions. The Fermi level is effectively pinned to the neutral defect level at low temperatures. In addition, our results seem to show that the defect centers are not related to any single conduction-band minimum. This model accounts well for measured temperature and pressure variations of the electron concentrations in  $\text{AEB}_6$ . However, the modeling of the magnetoresistance behavior becomes quite complex because of the variety of contributions and parameters it involves.

## II. EXPERIMENT

The single crystals of  $\text{AEB}_6$  used in our study were grown from Al flux with no intentional doping. The crystals were shaped into either thin platelets or prisms. All measurements were performed on small single crystals of approximately  $0.1 \times 0.5 \times 3 \text{ mm}^3$ . Prior to experiments, the crystals were cleaved and polished. We etched them in concentrated HCl acid before attaching contacts. Contact leads (25  $\mu\text{m}$  gold wire) were spot-welded to the samples. Low frequency transport measurements were carried out in helium cryostats with a six or four probe method. The resistivity and Hall effect were measured as a function of the magnetic field of up to 10 T. Clamp cells with a liquid (Daphne oil 7373) as a pressure-transmitting medium<sup>23</sup> were used for measurements under pressure of up to 30 kbar in a Quantum Design PPMS system. We have found no large sample to sample variations of the electrical parameters in any growth batch of  $\text{SrB}_6$  and  $\text{BaB}_6$  crystals. For  $\text{CaB}_6$ , on the other hand, these parameters are more sample-dependent.

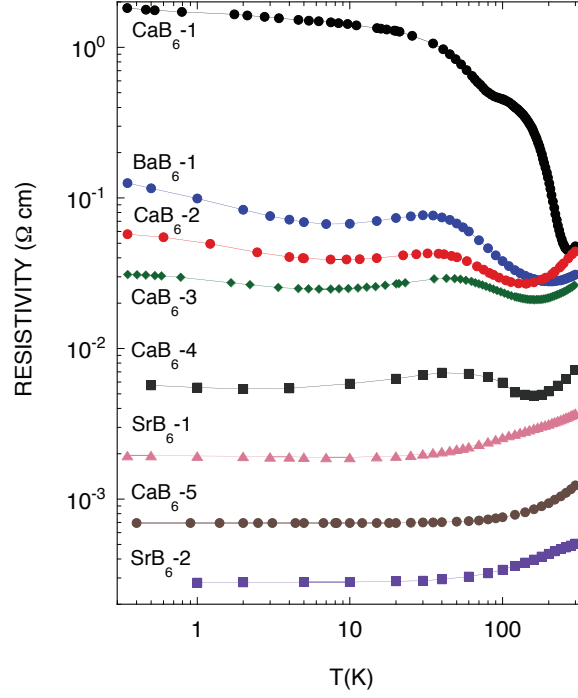


FIG. 1. (Color online) Variation of electrical resistivity with temperature for  $\text{AEB}_6$  (AE=Ca, Sr, Ba) single crystals.

TABLE I. Electrical transport parameters obtained for  $\text{AEB}_6$  (AE=Ca, Sr, Ba) single crystals from resistivity and Hall effect measurements.

Sample	$n(2 \text{ K})$ ( $\text{cm}^{-3}$ )	$\rho(2 \text{ K})$ ( $\Omega \text{ cm}$ )	$n(295 \text{ K})$ ( $\text{cm}^{-3}$ )	$\rho(295 \text{ K})$ ( $\Omega \text{ cm}$ )
$\text{CaB}_6\text{-1}$	$5.56 \times 10^{17}$	1.6310	$8.69 \times 10^{17}$	0.0478
$\text{BaB}_6\text{-1}$	$6.12 \times 10^{17}$	0.0835	$8.64 \times 10^{17}$	0.0305
$\text{CaB}_6\text{-2}$	$9.45 \times 10^{17}$	0.0448	$1.09 \times 10^{18}$	0.0442
$\text{CaB}_6\text{-3}$	$1.65 \times 10^{18}$	0.0268	$1.60 \times 10^{18}$	0.0263
$\text{CaB}_6\text{-4}$	$9.01 \times 10^{18}$	0.0054	$6.82 \times 10^{18}$	0.0071
$\text{SrB}_6\text{-1}$	$2.01 \times 10^{19}$	0.00267	$1.62 \times 10^{19}$	0.00515
$\text{CaB}_6\text{-5}$	$3.65 \times 10^{19}$	0.00069	$3.38 \times 10^{19}$	0.00123
$\text{SrB}_6\text{-2}$	$1.14 \times 10^{20}$	0.00022	$9.65 \times 10^{19}$	0.00040

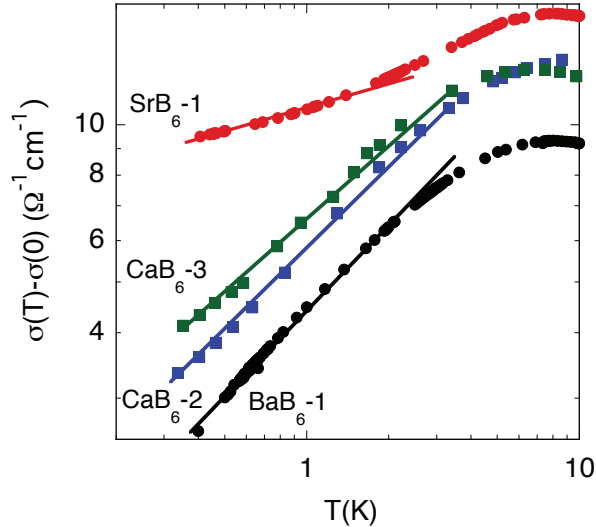


FIG. 2. (Color online) The difference between the conductivity and its extrapolated zero-temperature value is plotted *vs* temperature for some of AEB<sub>6</sub> single crystals. Below approximately 5 K, the power-law dependence has exponent 1/2

### III. RESULTS AND DISCUSSION

#### A. Temperature and pressure variation of resistivity and electron concentration

The variation of the electrical resistivity with temperature in stoichiometric AEB<sub>6</sub> single crystals is shown in Fig. 1. The differences in conductivity of these crystals arises from the self-doping. We found that the electronic transport is very similar for all alkaline earth cations in AEB<sub>6</sub> compounds we have studied. Table I gives values of electrical parameters at 2 and 295 K for samples discussed in this report.

Our measurements on different crystals show that the resistivity spans nearly five orders of magnitude. However, in each sample, the resistivity varies relatively little with temperature. As described in the previous report, upon lowering the temperature from 300 K, the resistivity  $\rho(T)$  first decreases, and subsequently increases in all but the more heavily doped crystals.  $\rho(T)$  shows another broad minimum at approximately 10 K in lightly doped crystals and increases at lower temperatures. At the lowest temperatures, we find that the conductivity  $\sigma \propto T^{1/2}$ . This is shown in Fig. 2 for some AEB<sub>6</sub> samples.

In Fig. 3 we plot the Hall resistivity  $\rho_H$  *vs* temperature. A broad maximum around 100 K is observed in  $\rho_H(T)$  for lightly doped samples. This maximum moves to higher temperatures as self-doping becomes larger. We found electron-type conduction for all of

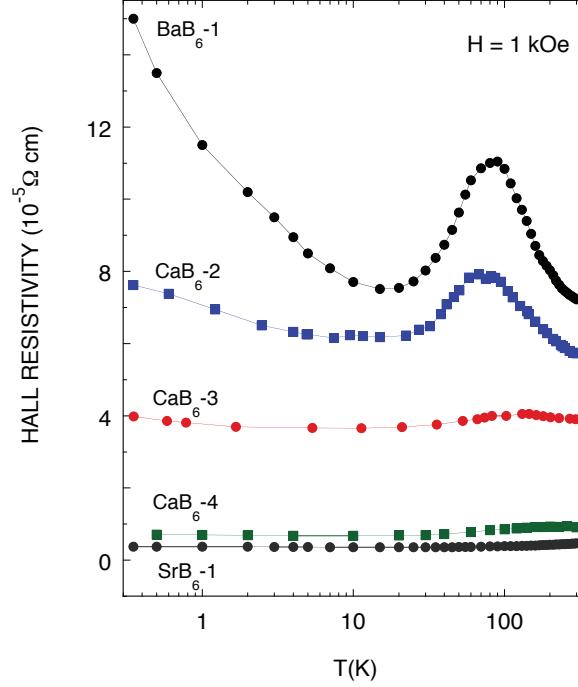


FIG. 3. (Color online) Variation of Hall resistivity with temperature for  $\text{AEB}_6$  (AE=Ca, Sr, Ba) single crystals.

our samples since  $\rho_H$  decreases linearly with the magnetic field (not shown), up to at least 5 T, in the temperature range we have studied. Figure 4 shows the dependence of the Hall coefficient  $R_H$  and the resistivity on the hydrostatic pressure  $p$  in some of the samples at two different temperatures. In general, the experimental results obtained under pressure do not change significantly with temperature for temperatures less than 100 K. For the lightly doped  $\text{BaB}_6$  single crystal,  $R_H$  drops initially with applied pressure and saturates beyond  $p \approx 8$  kbar, at both 80 and 300 K. For the  $\text{SrB}_6$  sample with much higher level of self-doping,  $R_H$  barely changes with  $p$  up to 25 kbar at  $T=80$  K. At higher temperatures, the Hall coefficient decreases with  $p$ . The results obtained for  $\text{CaB}_6$ -3 sample (not shown) are in line with this behavior.

The temperature variation of the Hall coefficient found in  $\text{AEB}_6$  single crystals is anomalous. The hump around or above 100 K cannot be accounted for by a simple impurity band contribution or other two-carrier models. To explain these results, we assume that the intrinsic defects form an impurity band which merges with the conduction band. Therefore, we have given positive charges to substitutional donors  $d^+$  which are in extended states. These centers may bind electrons and give rise to neutral localized centers  $d^0$  with energy

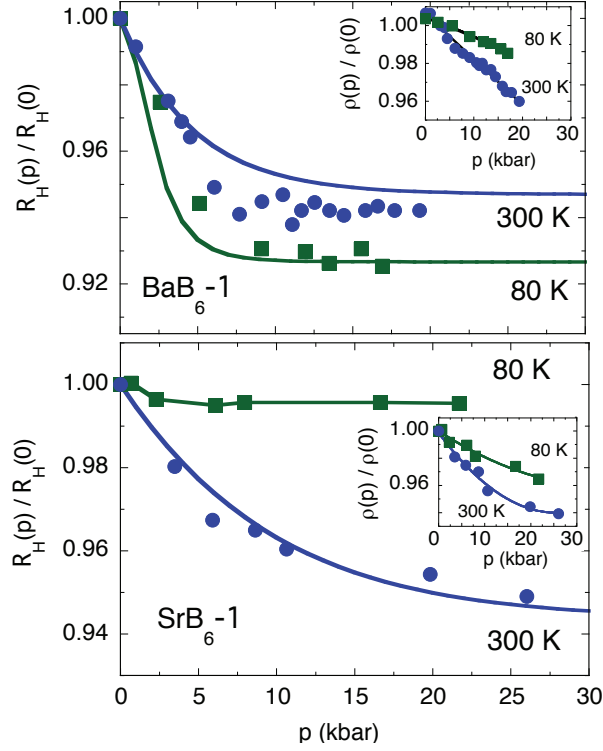


FIG. 4. (Color online) Hall coefficient dependence on hydrostatic pressure for BaB<sub>6</sub> (upper panel) and SrB<sub>6</sub> (lower panel) single crystals at two different temperatures. Solid lines are fits to experimental data points using the variable-valence defects model. The insets show how the resistivity for the above crystals varies with pressure.

$E_1$ . In addition, negatively charged localized donor states  $d^-$  at the energy  $E_2$  exist. In highly doped materials, these states may occur from the capture of two electrons by a donor ion according to the reaction:  $d^+ + 2e \rightarrow d^-$ .<sup>24</sup> The number of  $d^+$ ,  $d^0$ , and  $d^-$  states ( $n_+$ ,  $n_0$ , and  $n_-$ , respectively) is obtained from the statistics of multi-charged centers in semiconductors.<sup>25,26</sup> Accordingly,

$$n_+ = \frac{N_{def}}{1 + \frac{g_0}{g_+} e^{(\eta - \varepsilon_1)} + \frac{g_-}{g_+} e^{(2\eta - \varepsilon_2)}}; \quad (1)$$

$$n_0 = \frac{N_{def} \frac{g_0}{g_+} e^{\eta - \varepsilon_1}}{1 + \frac{g_-}{g_+} e^{(\eta - \varepsilon_1)} + \frac{g_-}{g_+} e^{(2\eta - \varepsilon_2)}}; \quad (2)$$

$$n_- = \frac{N_{def} \frac{g_-}{g_+} e^{2\eta - \varepsilon_2}}{1 + \frac{g_0}{g_+} e^{(\eta - \varepsilon_1)} + \frac{g_-}{g_+} e^{(2\eta - \varepsilon_2)}}; \quad (3)$$

where  $N_{def}$  is the total concentration of the native defects;  $g_i = g'_i e^{S_i/k_B}$ ,  $g'_i$  is the set of statistical weights for states  $i = +, 0$  and  $-$ , corresponding to the donor ion with no electron, with one electron, and with two electrons, respectively, and  $S_i$  is the vibrational



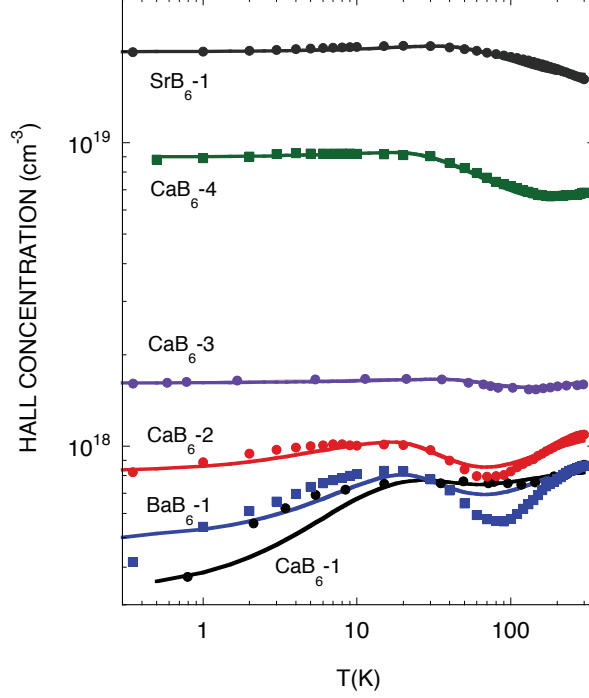


FIG. 5. (Color online) Hall electron concentration *vs* temperature for various AEB<sub>6</sub> single crystal samples. Solid lines are fits to experimental data points using the variable-valence defects model.

entropy of these states;  $\varepsilon_1 = E_1/k_B T$  and  $\varepsilon_2 = E_2/k_B T$  are the reduced energies of one and two electrons, respectively, and  $\eta = E_F/k_B T$ ,  $E_F$  is the energy of the Fermi level with respect to the bottom of the conduction band, and  $k_B$  is Boltzmann's constant. The electron concentration,  $n_{el}(T)$ , in the conduction band satisfies the neutrality condition:

$$n_{el} = N_I + n_+ - n_- \quad ; \quad (4)$$

where  $N_I = N_D - N_A$ ,  $N_A$  and  $N_D$  are the concentrations of additional acceptors and donors impurities in the crystals, respectively. Here, we assume the hole concentration in the valence band is negligible. The statistical weights for the three charge states of the defect are  $g'_i = 1, 2$ , and  $1$  ( $i = +, 0$ , and  $-$ ), respectively, if only the spin degeneracy is taken into account. The vibrational and configurational entropy content is more difficult to estimate. Although the contribution of localized impurities to the free electron energy is negligible in most cases,<sup>27</sup> we find that our fits improve assuming a small ( $\approx 3 \times 10^{-4}$  eV/K for the  $E_1$  state and  $10^{-5}$  eV/K for  $E_2$  state) entropy content.<sup>17</sup>

Figure 5 shows the variable-valence defects model fits of the measured temperature vari-

ation of the electron concentration ( $n_{el} = 1/eR_H$ ) in various AEB<sub>6</sub> single crystals. Our fitting parameters are:  $E_1$ ,  $E_2$ ,  $N_{def}$ , and  $N_I$ . The  $n_{el}$  is calculated by numerical integration of the standard density-of-state expression for a parabolic band with an effective mass of  $0.28m_o$  for CaB<sub>6</sub>,<sup>10</sup>,  $0.22m_o$  for BaB<sub>6</sub>,<sup>9</sup> and  $0.27m_o$  for SrB<sub>6</sub>.<sup>28</sup> Here,  $m_o$  is the free electron mass. The experimental behavior of the electron concentration, both for lightly and more heavily doped crystals, is reproduced rather well by our model. The Fermi level is effectively pinned to the  $E_1$  defect level at low temperatures. In Fig. 6 we plot the energies  $E_1$  and  $E_2$  as a function of the electron concentration in the conduction band. Since  $E_2$  is the energy of the two-electron state,  $E_2 > 2E_1$  at  $T=0$  is expected because of the electron-electron repulsion. The parameter  $U_{eff} = E_2 - 2E_1$  is also plotted in Fig. 6. It only depends weakly on  $n_{el}$  even though both  $E_1$  and  $E_2$  vary with  $n_{el}$  noticeably. This variation arises mainly from the mutual exchange and Coulomb interactions between the electrons which show up as an effective increase in the energy of the defects.<sup>29,30</sup> The Coulomb interactions among the electrons themselves lead to the lowering of the energy of the conduction band by approximately.<sup>29</sup>

$$\Delta E = -\frac{2e^2k_F}{\pi\epsilon}\left[1 + \frac{\pi\lambda}{2k_F} - \frac{\lambda}{k_F}\tan^{-1}\left(\frac{k_F}{\lambda}\right)\right]; \quad (5)$$

where  $k_F = (3\pi^2n/\nu)^{1/3}$  is the Fermi wave vector ( $\nu$  is the number of the conduction band minima),  $\epsilon$  is the dielectric constant ( $\epsilon \approx 6$ ),<sup>28</sup> and  $\lambda = (6\pi n_{el}e^2/\epsilon E_F)^{1/2}$  is the Thomas-Fermi screening parameter. The downward shift of the conduction band is further enhanced by the attractive interaction between the conduction carriers and the ionized  $d^+$  donors whose magnitude has been estimated as:  $\Delta E \approx -4\pi n_{el}e^2/\epsilon a_B\lambda^3$ , where  $e$  is the electron charge and  $a_B$  is the Bohr radius. In addition, the Coulomb interaction between negatively charged defect centers and conduction electrons may raise the defects' energy. All these corrections give a total of about 30 meV for  $n_{el} = 1 \times 10^{19} \text{ cm}^{-3}$  which agrees with our data. We note that  $E_2$  in Fig. 6 closely follows a  $n^{1/2}$  dependence pointing to the importance of conduction electron-impurity scattering. The values of  $E_1$ ,  $E_2$ ,  $N_{def}$ , and  $N_I$  are listed in Table II.

The fit to the Hall data could be improved by taking into account the many-valley nature of the conduction band in AEB<sub>6</sub> in the same way as has been done to explain the electrical transport anomalies of Sb-doped Ge.<sup>31</sup> The maxima in the resistivity and Hall

TABLE II. Energies of one ( $E_1$ ) and two electrons ( $E_2$ ) levels, concentration of the native defects  $N_{def}$ , and concentration of additional impurities  $N_I$  obtained from the fit of our model to the temperature variation of the electron concentration in AEB<sub>6</sub> (AE=Ca, Sr, Ba) single crystals.

Sample	$E_1$ (eV)	$E_2$ (eV)	$N_{def}$ (cm <sup>-3</sup> )	$N_I$ (cm <sup>-3</sup> )
CaB <sub>6</sub> -1	0.0030	0.018	$7.3 \times 10^{17}$	$1.0 \times 10^{17}$
BaB <sub>6</sub> -1	0.0035	0.019	$9 \times 10^{17}$	0
CaB <sub>6</sub> -2	0.0055	0.018	$1.1 \times 10^{18}$	0
CaB <sub>6</sub> -3	0.0086	0.029	$1.5 \times 10^{18}$	$2.0 \times 10^{17}$
CaB <sub>6</sub> -4	0.027	0.040	$7.2 \times 10^{18}$	$2.5 \times 10^{18}$
SrB <sub>6</sub> -1	0.046	0.067	$2.1 \times 10^{19}$	$1.0 \times 10^{18}$
CaB <sub>6</sub> -5	0.068	0.096	$3.2 \times 10^{19}$	$5.5 \times 10^{18}$
SrB <sub>6</sub> -2	0.155	0.180	$8.3 \times 10^{19}$	$2.95 \times 10^{19}$

coefficient, observed at  $T \approx T_F$  ( $T_F$  is the Fermi temperature), have been attributed to strong electron scattering when the temperature-dependent Thomas-Fermi screening parameter ( $k_{TF}$ ) becomes comparable to the Fermi wave-vector in this many-valley semiconductor.<sup>32</sup> For single-valley cases, the range of the scattering potential is always larger than the Fermi wave-length and such enhancement of scattering does not happen. Pertinent calculation involves various approximations in order to take into account nonlinear screening, many-body effects, and multiple scattering. In addition, it requires knowledge of many band parameters which, at present, are not well established for AEB<sub>6</sub> compounds. All of these prevented us from performing this task.

Further support for our variable-charge defect model comes from experiments under hydrostatic pressure. The observed drop of  $R_H$  versus  $p$  (see Fig. 4) can only be brought about by the rise in energy of the defect levels with respect to the minimum of the conduction band and, consequently, their depopulation. The solid lines in Fig. 4 show the calculated variation of the Hall coefficient  $R_H$  with  $p$  using the parameters deduced above and a value of 3 meV/kbar for  $dE_1/dp$  and  $dE_2/dp$ . We assume  $dE_1/dp = dE_2/dp$  since nearly the same values of these coefficients have been found for other compounds.<sup>37</sup> The model fits the experimental data very well for the all compounds we have studied. The increase of the energy of the defects could be attributed to the downward pressure shift of the X-point conduction minimum, as had been suggested for EuB<sub>6</sub>.<sup>33</sup> However, such conjecture disagrees

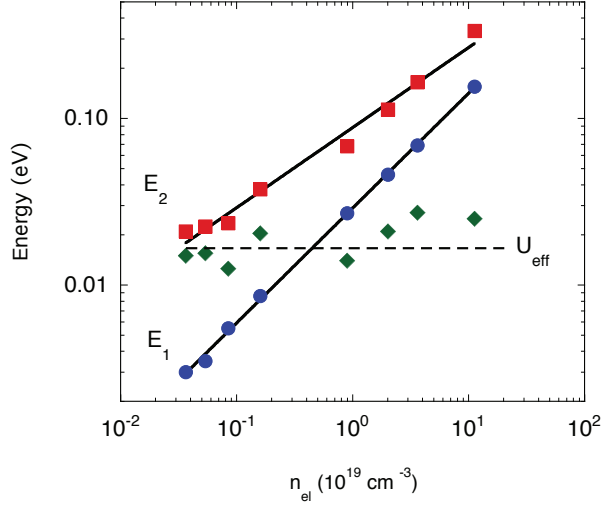


FIG. 6. (Color online) Fitting parameters  $E_1$  (circles) and  $E_2$  (squares) *vs* electron concentration in AEB<sub>6</sub> single crystals.  $U_{eff} = E_2 - 2E_1$  is the energy of on-site repulsion (rhombus). Solid and dotted lines are to guide an eye.

with the experimental observation that the inter-band energy gaps increase with pressure.<sup>34</sup> Furthermore, recent high-pressure synchrotron x-ray diffraction studies of BaB<sub>6</sub> show a decrease of the lattice constant pointing to an increase with pressure of the energy gap in this compound.<sup>35</sup> Therefore, some other mechanism should lie behind this effect. In addition, our results seem to show that the localized defect centers are not related to any single conduction-band minimum since its variation with pressure differs considerably from the shifts of the  $\Gamma$  or  $X$  points. We find that neither the energy nor the pressure coefficient of the localized defects centers vary significantly with temperature.

The question arises if the localized levels we infer from electrical transport measurements are coupled to the lattice and, therefore, metastable.<sup>36,37</sup> To this end we performed Hall effect and resistivity measurements illuminating the CaB<sub>6</sub>-3 sample at low temperatures with an IR LED, operating at a wavelength of about 910 nm. A small (about 2%) increase has been observed in  $R_H$  only when the illumination was on and for  $T < 30$  K. Under these conditions, the resistivity becomes larger, by approximately the same amount. Interestingly, a very weak negative magnetoresistance below approximately 2 kOe appears. None of these effects is persistent. Thus, we conclude that defect-lattice coupling is not important in AEB<sub>6</sub>.

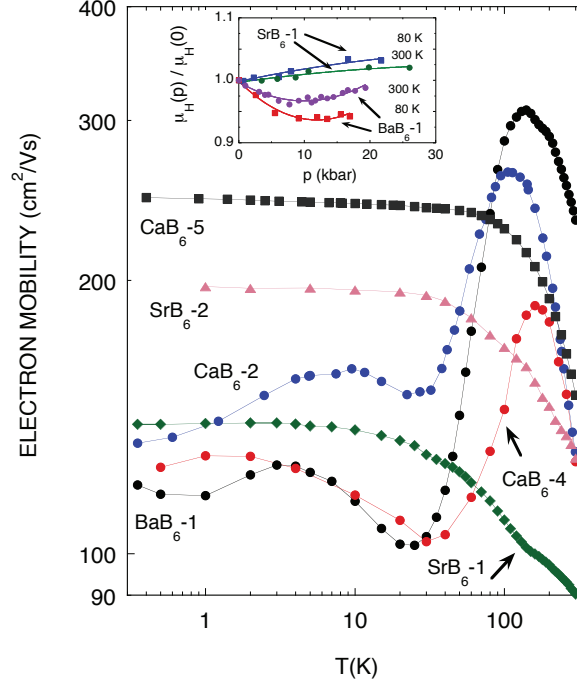


FIG. 7. (Color online) Temperature variation of the Hall mobility for AEB<sub>6</sub> single crystals. The inset shows how the mobility changes with pressure for two samples.

## B. Temperature and pressure variation of mobility

Figure 7 shows the temperature dependence of the low-field Hall mobility, obtained from  $\mu_H = R_H/\rho$ . For crystals with less than  $10^{19}$  defects per  $\text{cm}^{-3}$ , the mobility first increases with decreasing temperature. Below approximately 150 K, it drops rapidly and goes through a shallow minimum to a nearly constant value at low temperatures. In the more resistive samples,  $\mu_H$  drops (below  $10 \text{ cm}^2/\text{Vs}$ ) to quite small values at low temperatures. In heavily doped crystals, the Hall mobility is constant for  $T \lesssim 80 \text{ K}$  and decreases at higher temperatures.

Carrier mobilities in a moderately doped semiconductor are usually limited by electron-phonon scattering and, at lower temperatures, by ionized impurity scattering. Close to room-temperature, the mobility in our crystals varies as  $T^{-3/2}$ . From this, we infer that acoustic phonon scattering limits the mobility. On the other hand, the anomalous variation of the mobility at lower temperatures does not follow impurity scattering. We argue that the observed behavior can perhaps be explained by a resonant scattering of electrons by defects. It has been shown that substitutional impurities with a large central-cell potential

can give rise to levels above the conduction-band edge in semiconductors.<sup>38</sup> Such levels are narrow resonances because there is mixing with the conduction-band states. An electron at the energy of a resonance suffers strong scattering that can dominate other scattering mechanisms if the resonant level lies close enough to the conduction-band minimum.<sup>39</sup> It seems therefore plausible that the drop in mobility observed in lightly doped crystals is brought by the central-cell potential of resonant defects. As the localized levels of the defects move up in the conduction-band with increasing self-doping level, the central-cell scattering cross-section becomes smaller and other mechanisms start to dominate. For this reason, we do not observe a resonant effect in heavily doped crystals. It is worth to mention that muon spin relaxation experiments show a significant change in the electronic states of  $\text{CaB}_6$  and  $\text{BaB}_6$  below  $\approx 130$  K, much like the resonant scattering effect observed in alkaline-earth hexaborides.<sup>40</sup>

The inset in Fig. 7 shows the variation of the Hall mobility in  $\text{AEB}_6$  single crystals with pressure. We observe that  $\mu_H$  increases with increasing pressure for the  $\text{SrB}_6$ -1 single crystal at 2 K. The carrier concentration for this sample does not change with pressure. On the other hand,  $\mu_H$  slowly decreases upon applying pressure in the  $\text{BaB}_6$ -1 crystal for which  $n_{el}$  increases with  $p$ . To interpret these results, we will consider the ionized impurity scattering since this mechanism limits electron mobility at low temperatures. Within the Born approximation for strongly degenerated materials, the mobility is proportional to:<sup>41</sup>  $\mu \propto \epsilon^2(n_{el}/N_I)(1/m^*(E_F))^2(1/F(\lambda, E_F))$ , where  $m^*(E_F)$  is the effective mass, evaluated at the Fermi surface, and  $F(\lambda, E_F)$  is the scattering function. Other symbols are defined above. For the case when the applied pressure does not affect  $n_{el}$ , the pressure-induced changes of the dielectric constant would lead to the observed rise of the electron mobility.<sup>42</sup> On the other hand, the rise in the carrier density under pressure leads to the increase of  $E_F$ , and of  $m^*(E_F)$ . As the scattering function also becomes larger, the mobility decreases with pressure. However, taking into account the variation of the  $n_{el}/N_I$  term in the expression for the mobility may reverse this trend. We expect that the number of charged defects  $N_I$  does not change significantly with pressure since in our crystals the rate for the two-electron capture by the  $d^+$  center and subsequent formation of  $d^-$  states is higher than the rate for capture of electrons by  $d^+$  states and subsequent formation of neutral states  $d^0$ . Therefore, the variation of the  $n_{el}/N_I$  counterbalances the decrease in mobility brought by the band effects and starts to dominate for high pressures. The  $\mu_H(p)$  behavior at 80 K for  $\text{BaB}_6$ -1

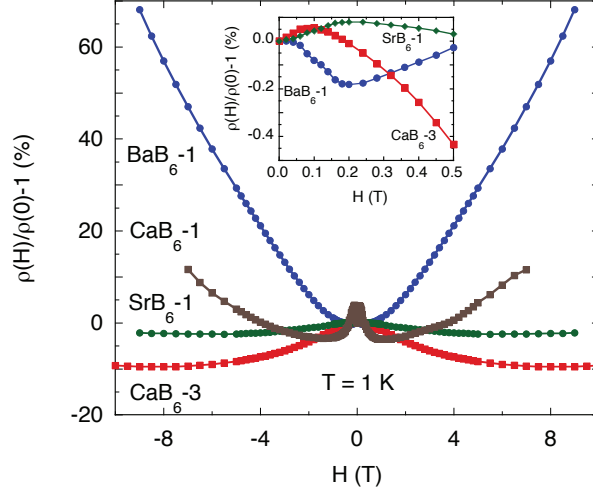


FIG. 8. (Color online) Low-temperature magnetoresistance for AEB<sub>6</sub> single crystals in different localization regimes. The low-field region is shown in the inset.

crystal, shown in Fig. 7, is consistent with these predictions.

### C. Magnetoresistance

The single crystals we study are self-doped intrinsic semiconductors. When the defect concentration is large enough, there is an insulator-metal (MI) transition arising from shallow impurity-state overlap. A sharp drop in low-temperature Hall mobility at  $n_{el} \approx 1 \cdot 10^{18} \text{ cm}^{-3}$ , which we reported for CaB<sub>6</sub> crystals,<sup>20</sup> corresponds to the MI transition in this system. The product  $k_F l$ , where  $l = (\hbar/e)k_F \mu$  is the mean free path, is frequently used to assess the conduction regime of the material. We find that for lightly doped samples,  $k_F l$  is much smaller than 1, which suggests a strongly localized regime. Most of our crystals however are either in the critical region ( $k_F l \simeq 1$ ) or on the metallic side of the MI transition in a weakly localized regime (WLR), for which  $k_F l > 1$ .

Our discussion of the MR in AEB<sub>6</sub> single crystals is mainly based on localization and Coulomb interaction models for disordered systems.<sup>43</sup> The localization term lowers conductivity as temperature decreases. On the other hand, Coulomb interactions give a temperature correction to  $\sigma(0)$  of the form  $\sqrt{T}$  that can change sign as the screening length varies.<sup>44</sup> In particular, electron-electron scattering at low temperatures leads to  $\sigma(T) = \sigma(0)[1 + fA(T/T_o)^{1/2}]$ .<sup>45</sup> Here,  $A = 0.72$ ,  $T_o$  is a characteristic temperature  $T_o = T_F(k_F l)^3$ , and  $f = 1 - (3/2x)\ln(1+x)$ , where  $x = 2k_F/k_{TF}$ .<sup>46</sup> For the crystals we have studied,  $x$

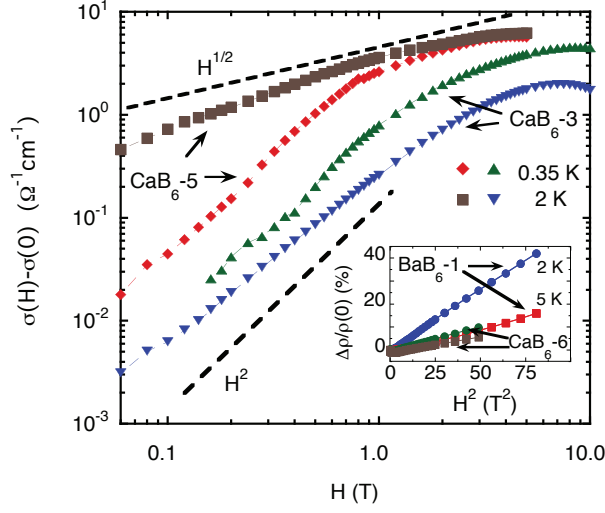


FIG. 9. (Color online) Low-temperature magneto-conductance for  $\text{CaB}_6$  single crystals in the weakly localized regime. The inset shows magnetoresistance as a function of the square of the magnetic field for the crystals in strongly localized and critical regime.

varies between 1 and 2, which renders  $f$  positive, in agreement with the data plotted in Fig. 2. Therefore, the low-temperature variation of the conductivity in our samples most likely arises from Coulomb interactions.

As mentioned above, multiple scattering (localization) can give rise to a drop in the conductivity for metallic samples.<sup>47</sup> Since the magnetic field  $H$  suppresses localization, negative magnetoresistance (MR) is often observed at high magnetic fields.<sup>48</sup> On the other hand, spin-orbit scattering can lead to negative corrections to  $\sigma(T)$  through destructive-interference effects<sup>49</sup> and, therefore, to positive MR.<sup>43</sup> This effect should, in principle, be observed for compounds with high atomic number.<sup>50</sup> Furthermore, Zeeman splitting can also be important for positive MR in metallic samples under certain conditions.<sup>51</sup>

Our MR measurements on  $\text{AEB}_6$  single crystals show both positive and negative components. This is displayed in Fig. 8. Let us first discuss the negative MR which we observe for crystals in the WLR. When  $H$  is not very strong, the magnetic length  $l_h \equiv (c\hbar/eH)^{1/2} \gg l$ , and at low temperatures, the leading term in magnetoconductivity,  $\Delta\sigma = \sigma(H) - \sigma(0)$ , comes from the localization effect. It has a simple form:  $\Delta\sigma(H, 0) = 2.90\sqrt{H}$ , where  $\Delta\sigma$  is in units of  $\Omega^{-1}\text{cm}^{-1}$  for  $H$  given in Tesla.<sup>52</sup> For weak magnetic fields,  $\Delta\sigma \propto H^2$ . The data plotted in Fig. 9 seem to follow these predictions. We find that  $\Delta\sigma \approx 3.5\sqrt{H}$  at intermediate fields. This is larger than the theoretical value of 2.9. The difference most likely comes from the anisotropy of the Fermi surface in  $\text{CaB}_6$ .<sup>52</sup> Enhanced electron interactions in the presence



of orbital and spin splitting effects in WLR lead to a positive MR.<sup>49,53</sup> This is observed at weak magnetic fields as shown for SrB<sub>6</sub>-1 and CaB<sub>6</sub>-3 crystals in the inset of Fig. 8. Generally, electron interaction corrections are much smaller than the negative localization effect.

The crystals in the critical or strongly localized regime show a positive MR, as displayed in the inset of Fig. 9 for two samples. We find a quadratic dependence of the MR on applied magnetic field, as in the classical description of the Hall effect. However, the classical effect is usually rather small, and is often masked by other contributions to the MR. Hopping conduction in the impurity band gives rise to an exponential dependence of the resistivity on temperature and magnetic field which comes from diamagnetic shrinking of the wave function.<sup>54,55</sup> We do not observe such behavior in our samples. We believe that the paramagnetic splitting of the conduction band and of the  $d^0$  defect level is a likely explanation.<sup>51</sup> At the highest applied fields (near 10 T), this splitting is less than 1 meV for free electrons. Therefore, the Zeeman effect raises the density of states at the Fermi level only marginally for one spin band and lowers it for the other. Even so, its effect on the electron concentrations at low temperatures accounts to 0.2% in samples with  $\approx 10^{19}$  defects per cm<sup>-3</sup> and gives higher values for lightly doped crystals. Furthermore, including the splitting of the  $d^0$  level leads to larger variations of  $n_{el}$  with magnetic field. Consequently, the modeling of the MR behavior becomes quite complicated because of the various contributions and parameters it involves.

#### IV. CONCLUSIONS

In summary, we have consistently explained the variation of the electrical resistivity and the Hall effect with temperature and hydrostatic pressure in AEB<sub>6</sub> single crystals. This is achieved with a variable-charge defect model. The defects are intrinsic to all the alkaline hexaborides we have studied. They give rise to a narrow band, resonant with the conduction band, which effectively pins the Fermi level at low temperatures. In addition, a negatively charged, localized level of the same defect exists at a higher energy level. This situation leads to a weak temperature and pressure variation of the electron concentration and mobility in AEB<sub>6</sub> systems.

The low-temperature variation of the conductivity in these systems most likely arises

from Coulomb interactions. These interactions are also responsible for a small positive magnetoresistance which we observe at low magnetic fields, for samples in a weakly localized regime. A negative MR, which shows up at higher magnetic field in heavily doped crystals, follows from localization effects. Lightly doped samples exhibit a large positive magnetoresistance that is difficult to model because of the variety of contributions involved.

We acknowledge support from grant MAT2012-38213-C02-01, from the Ministerio de Economía y Competitividad of Spain. Additional support from Diputación General de Aragón (DGA-CAMRADS) is also acknowledged. Work at Los Alamos was performed under the auspices of the U.S. Department of Energy, Office of Basic Energy Sciences, Division of Materials Science and Engineering. P. F. S. R. acknowledges a Director's Postdoctoral Fellowship through the LANL LDRD program. P. S. acknowledges the support by the US Department of Energy (BES) under grant No. DE-FG02-98ER45707. We used Servicio General de Apoyo a la Investigación (SAI) of Universidad de Zaragoza in our research.

- 
- <sup>1</sup> D. P. Young, *et al.*, Nature **397**, 412 (1999).
  - <sup>2</sup> H. R. Ott, *et al.*, Physica B **281-282**, 423 (2000).
  - <sup>3</sup> D. M. Edwards and M. I. Katsnelson, J. Phys.: Condens. Matter **18**, 7209 (2006).
  - <sup>4</sup> K. Maiti, Eur. Phys. Lett. **82**, 67006 (2008).
  - <sup>5</sup> M. Li, H. Wang, K. Snoussi, L. Li, W. Yang, and Ch. Gao, J. Appl. Phys. **108**, 103710 (2010).
  - <sup>6</sup> Y. Li, J. Yang, X. Cui, T. Hu, C. Liu, Y. Tian, H. Liu, Y. Han, and Ch. Gao, Phys. Stat. Sol. B **248**, 1162 (2011).
  - <sup>7</sup> A. N. Kolmogorov, S. Shah, E. R. Margine, A. K. Kleppe, and A. P. Jephcoat, Phys. Rev. Lett. **109**, 075501 (2012).
  - <sup>8</sup> G. Zhao, L. Zhang, L. Hu, H. Yu, G. Min, and H. Yu, J. Alloys and Compounds **599**, 175 (2014).
  - <sup>9</sup> S. Massidda, A. Continenza, T.M. Pascale, R. Monnier, Z. Phys. B **102**, 83 (1997); S. Massidda, R. Monnier, and E. Stoll, Eur. Phys. J. B **17**, 645 (2000).
  - <sup>10</sup> H. J. Tromp, P. van Gelderen, P. J. Kelly, G. Brocks, and P. A. Bobbert, Phys. Rev. Lett. **87**, 016401 (2000).
  - <sup>11</sup> B. Lee and L-W. Wang, Appl. Phys. Lett. **87**, 262509 (2005).

- <sup>12</sup> J. D. Denlinger, J. A. Clack, J. W. Allen, G.-H. Gweon, D. M. Poirier, C. G. Olson, J. L. Sarrao, A. D. Bianchi, and Z. Fisk, Phys. Rev. Lett. **89**, 157601 (2002).
- <sup>13</sup> S. Souma, H. Komatsu, T. Takahashi, R. Kaji, T. Sasaki, Y. Yokoo, and J. Akimitsu, Phys. Rev. Lett. **90**, 027202 (2003).
- <sup>14</sup> K. Giannó, A. V. Sologubenko, H. R. Ott, A. D. Bianchi, and Z. Fisk, J. Phys.: Condens. Matter **14**, 1035 (2002).
- <sup>15</sup> Z. Fisk, H.R. Ott, V. Barzykina, and L.P. Gor'kov, Physica B **312-313**, 808 (2002).
- <sup>16</sup> S. Paschen, D. Pushin, M. Schlatter, P. Vonlanthen, H. R. Ott, D. P. Young, and Z. Fisk, Phys. Rev. B **61**, 4174 (2000).
- <sup>17</sup> P. Vonlanthen, E. Felder, L. Degiorgi, H. R. Ott, D. P. Young, A. D. Bianchi, and Z. Fisk, Phys. Rev. B **62**, 10076 (2000).
- <sup>18</sup> H. R. Ott, M. Chernikov, E. Felder, L. Degiorgi, E.G. Moshopoulou, J.L. Sarrao, and Z. Fisk, Z. Phys. B **102**, 337 (1997).
- <sup>19</sup> R. Monnier and B. Delley, Phys. Rev. Lett. **87**, 157204 (2001).
- <sup>20</sup> J. Stankiewicz, J. Sesé, G. Balakrishnan, and Z. Fisk, Phys. Rev. B **90**, 155128 (2014).
- <sup>21</sup> J. Friedel, Can. J. Phys. **34**, 1190 (1956).
- <sup>22</sup> J. P. Heremans, B. Wiendlocha, and A. M. Chamoire, Energy Environ. Sci. **5**, 5510 (2012).
- <sup>23</sup> ElectroLAB Company, Chiba, Japan.
- <sup>24</sup> D. J. Chadi and K. J. Chang, Phys. Rev. B **39**, 10063 (1989).
- <sup>25</sup> W. Shockley and J. T. Last, Phys. Rev **107**, 392 (1957).
- <sup>26</sup> D. C. Look, Phys. Rev. B **24**, 5852 (1981).
- <sup>27</sup> S. K. Estreicher, M. Sanati, D. West, and F. Ruymgaart, Phys. Rev. B **70**, 125209 (2004).
- <sup>28</sup> C. O. Rodriguez, R. Weht, and W. E. Pickett, Phys. Rev. Lett. **84**, 3903 (2000).
- <sup>29</sup> K.-F. Berggren and B. E. Sernelius, Phys. Rev. B **24**, 1971 (1981).
- <sup>30</sup> R. A. Abram, G. J. Rees, and B. L. H. Wilson, Adv. Phys. **27**, 799 (1978).
- <sup>31</sup> T. Kurosawa, M. Matsui, and W. Sasaki, J. Phys. Soc. Jpn. **42**, 1622 (1977).
- <sup>32</sup> T. Saso and T. Kasuya, J. Phys. Soc. Jpn. **48**, 1566 (1980).
- <sup>33</sup> G. Weill, I.A. Smirnov and V.N. Gurin, J. de Physique **41**, C5-185 (1980).
- <sup>34</sup> R. Zallen and W. Paul, Phys. Rev. **155**, 703(1967).
- <sup>35</sup> X. Li, X. Huang, D. Duan, G. Wu, M. Liu, Q. Zhuang, S. Wei, Y. Huang, F. Li, Q. Zhou, B. Liu, and T. Cui, RSC Adv. **6**, 18077 (2016).

- <sup>36</sup> P. M. Mooney, J. Appl. Phys. **67**, R1 (1990).
- <sup>37</sup> T. Suski, R. Piotrkowski, P. Wisniewski, E. Litwin-Staszewska, and L. Dmowski, Phys. Rev. B **40**, 4012 (1989).
- <sup>38</sup> H. P. Hjalmarson, P. Vogl, D. J. Welford, and J. D. Dow, Phys. Rev. Lett. **44**, 80 (1980).
- <sup>39</sup> O. F. Sankey, J. D. Dow, and K. Hess, Appl. Phys. Lett. **41**, 664 (1982).
- <sup>40</sup> S. Kuroiwa, H. Takagiwa, M. Yamazawa, J. Akimitsu, A. Koda, R. Kadono, K. Ohishi, W. Higemoto, and I. Watanabe, Sci. Technol. Adv. Mater. **7**, 12 (2006).
- <sup>41</sup> W. Zawadzki, in *Handbook of Semiconductors*, edited by W. Paul (North-Holland, Amsterdam, 1982), Vol. 1, p. 725.
- <sup>42</sup> Z. Wasilewski and R. A. Stradling, Semicond. Sci. Technol. **1**, 264 (1986).
- <sup>43</sup> P. A. Lee and T. V. Ramakrishnan, Rev. Mod. Phys. **57**, 287 (1985).
- <sup>44</sup> T. F. Rosenbaum, K. Andres, G. A. Thomas, and P. A. Lee, Phys. Rev. Lett. **46**, 568 (1981).
- <sup>45</sup> B. L. Altshuler and A. G. Aronov, Zh. Eksp. Teor. Fiz. **77**, 2028 (1979) [Sov. Phys. JETP **50**, 968 (1979)]; Solid State Commun. **36**, 115 (1979).
- <sup>46</sup> B. L. Altshuler, A. G. Aronov, and P. A. Lee, Phys. Rev. Lett. **44**, 1288 (1980).
- <sup>47</sup> G. Bergmann, Phys. Rep. **107**, 1 (1984).
- <sup>48</sup> A. Kawabata, J. Phys. Soc. Japan **49**, 628 (1980).
- <sup>49</sup> H. Fukuyama and K. Hoshino, J. Phys. Soc. Jpn. **50**, 2131 (1981).
- <sup>50</sup> N. F. Mott, in *Metal-Insulator transitions*, (Taylor & Francis, London, 1990).
- <sup>51</sup> G. Xiong, Sh-D. Wang, and X. R. Wang, Phys. Rev. B **61**, 14335 (2000).
- <sup>52</sup> Y. Ootuka and A. Kawabata, Prog. Theor. Phys., Suppl. **84**, 249 (1985).
- <sup>53</sup> B. L. Altshuler, and A. G. Aronov, in *Electron-Electron Interactions in Disordered Systems*, edited by M. Pollak and A. L. Efros, North-Holland, Amsterdam (1985).
- <sup>54</sup> B. I. Shklovskii and A. L. Efros, in *Electronic Properties of Doped Semiconductors* Springer-Verlag, New York (1984).
- <sup>55</sup> D. M. Finlayson, J. Irvine, and L. S. Peterkin, Phil. Mag. B **39**, 253 (1979).